

PATH CORRECTIONS FOR REGIONAL PHASE DISCRIMINANTS

Thorne Lay, Guangwei Fan, Ru-Shan Wu, Xiao-bi Xie

Earth Sciences Department and Institute of Tectonics
University of California, Santa Cruz

Sponsored by Defense Threat Reduction Agency

Contract No. DSWA01-98-C-0161-P00001

ABSTRACT

In order to utilize regional seismic phases for reliable source identification, it is essential to account for wave propagation effects that may obscure the subtle differences in source radiation for distinct source types. Recent work has established three main approaches to the problem of characterizing and correcting regional phases for propagation effects: empirical methods based on parametric dependence on path properties such as pathlength or crustal waveguide parameters, interpolation methods such as cap-averaging and kriging for station-dependent source region correction surfaces, and waveform modeling methods based on complete waveform synthesis for two-dimensional or three-dimensional crustal models. Our research program is exploring all three approaches, seeking to establish relative merits of each strategy for different situations. In a recent publication we compare the reduction in scatter for regional P/S amplitude ratios for station ABKT for distance correction, waveguide parameter regressions, cap-averaging, and kriging (Rodgers et al., 1999), finding that kriging has some distinct advantages over other methods. We have further explored kriging and waveguide parameter regressions for two International Seismic Monitoring Stations, NIL and ZAL. Frequency dependent regional phase amplitude ratio measurements at these stations for earthquakes and underground nuclear explosions, obtained from the Comprehensive Nuclear-Test-Ban Treaty prototype-International Data Center, have a large amount of scatter, most of which is attributed to wave propagation effects in the heterogeneous crustal waveguide. Interpolation of the anomalies using a Kriging algorithm achieves significant variance reduction, but provides little insight into the nature of the path effects. Linear regressions indicate that the phase ratios are correlated with topographic features along the paths, providing an empirical means for reducing path effects beyond conventional distance corrections. Topography variations appear to provide a proxy for structural complexity of the crustal waveguide, which influences the reverberations and energy partitioning in the regional wavefield in a way that can be statistically isolated. Using available high-resolution topography data, correction of regional P/S ratios for the best models obtained from multivariate regressions systematically reduces the data variance relative to path length corrections alone, as has been observed for other data sets. The reduced scatter in the measurements increases the separations between earthquake and explosion populations in most cases, enhancing the regional discriminant performance. The path-corrected discriminants work better at station NIL than at station ZAL, even though the explosion sources are located in a common source area. The laterally varying characteristics of the waveguide structure for different sets of paths can apparently overwhelm intrinsic source differences, complicating discrimination when small numbers of observations are available. While always desirable, corrections for heterogeneous path effects may prove inadequate in some cases, notably when phase blockage occurs or when strong attenuation reduces the diagnostic high frequency energy. Our modeling approach is based on breakthrough developments by our group in long-range high frequency regional wave synthesis, using half-space screen propagators. We analyze Lg signals for paths traversing the Tibetan Plateau using spectrograms to characterize the frequency dependent transmission effects, and then synthesize two-dimensional seismograms for plausible crustal models. An observed increase in Lg spectral ratios for the 3-6Hz/0.75-1.5Hz bands with propagation distance within the Plateau can be explained if we assume that small-scale random heterogeneity and/or random rough topography at the surface and layer interfaces is present. The complex-screen propagator method is used to generate synthetic Lg up to 10 Hz over paths as long as 1000 km.

Key Words: seismic discriminants, regional seismic phases, amplitude corrections, regional wave propagation

OBJECTIVE

One of the major challenges confronting seismic monitoring of the Comprehensive Nuclear-Test-Ban Treaty (CTBT) is discriminating the seismic signals of small underground explosions from those produced by other sources. There is tremendous regional variability in short-period signals from all sources, and the characteristics that define the source type may be subtle, easily overwhelmed by propagation complexities in the heterogeneous crust. Reliable regional seismic discriminants must have sufficiently small scatter in the background earthquake population that rare single-shot explosion events will produce diagnostic outlying measurements. That component of the scatter caused by propagation effects can be reduced by path corrections of varying sophistication. We are seeking to develop and test various approaches to reduce the scatter in regional discriminant populations, using numerous observations in Eurasia (China, Russia, and Southeast Asia, in particular) and the Middle East collected under this and a previous PL/DOE-funded effort. Multi-variate regressions of various path attributes (to assess which parametric path characterizations are significant), spatial representations of the path influences such as kriging (to enable interpolation to a unique path for a suspect event), and tests of significance of the corrections (ability to tighten up scatter in discriminant measures to a useful extent) are all being considered in our effort to develop a unified strategy for discriminant calibration that will transport into the operational regime and lead to high confidence discrimination.

RESEARCH ACCOMPLISHED

Our first year of research has addressed improving the performance of short-period regional seismic discriminants by applying propagation corrections to regional P/S amplitude ratios observed at two seismic monitoring stations in Asia, NIL (Nilore, Pakistan) and ZAL (Zalesovo, Russia), which are part of the ISMS. The regional phase amplitude ratios recorded at these stations are correlated with regionally-averaged distance effects as well as path-specific effects parameterized by measures of surface topography. A high-resolution topographic database is used because the most reliable waveguide parameters available for any path are those involving surface topography. We consider path-integrated properties (e.g., mean altitude, average surface roughness, etc.) because regional wave propagation effects are likely to involve significant lateral averaging. For comparison, ordinary Kriging, which involves multiple regression on spatial parameters, is utilized to estimate path corrections and to visualize the systematic regional path effects. We test whether the reduced scatter in the regional seismic discriminant measures for NIL and ZAL using the topographic models actually yields better separation between earthquake and explosion populations. We also explore whether regionally distinctive characteristics of waveguide structure and geologic setting influence source discrimination performance.

Central Asia is a region of significant interest for monitoring the CTBT. Diffuse seismicity, sparse seismic instrumentation, acute crustal heterogeneity, and recent nuclear testing prioritize the area as a target for calibration of regional discriminants. Observed broadband waveforms for paths in Eurasia display great complexity (e.g., Zhang *et al.*, 1994), presumably caused by a combination of lateral heterogeneity in waveguide structure and source radiation effects. Our data set involves broadband vertical component recordings at ISMS stations NIL and ZAL for Eurasian earthquakes with magnitudes of $3.5 \leq m_b \leq 6.0$ that occurred between 1995 and 1998. Hypocenter parameters are those determined by the CTBT prototype-International Data Center (pIDC). The sparse ISMS station coverage and the complexity of the crustal and upper mantle structure in the region result in large uncertainties for hypocenter parameters, especially for focal depth, thus many smaller events assigned zero depth in the pIDC location are not well-constrained. We only consider shallow events, with pIDC focal depth estimates less than 50 km. The locations are otherwise deemed sufficient for the path property measurements used in this study, and the location uncertainties are typical of those for discriminant calibration efforts in all regions.

We use the amplitude measurements routinely made by the pIDC. The pIDC algorithm processes regional phases using the Detection and Feature Extraction (DFX) code, computing many amplitude measurements for a variety of filtered traces for specified time windows. Time windows are based on either a predicted travel time for a specific phase, a fixed group velocity window, or some combination of the two. The Pn amplitude is calculated within a window starting 8 s before the theoretical arrival time and ending at a group velocity of 6.4 km/s; the Sn window starts 5 s before the theoretical arrival time and has a duration of 20 s. The Pg and Lg windows are between group velocities of 6.3 to 5.8 km/s and 3.7 to 3.0 km/s, respectively. The precise pIDC windows differ from the corresponding windows used in many prior studies of regional discriminants (e.g., Walter *et al.*, 1995; Hartse *et al.*, 1997; Fan and Lay, 1998a, b), so some caution in comparison of results is warranted. The default windows can result in some spurious amplitude measurements in regions of strong crustal heterogeneity as well as varying proportion of coda contribution with distance, but one of our objectives was to exercise the database

generated routinely by the pIDC, as this will ultimately underlie operational applications. In particular, at small epicentral distances there is great difficulty in regional phase isolation, thus only signals at distances greater than 280 km were analyzed. Measurements out to 2100 km were used, recognizing that upper mantle P and S wave triplications overprint true regional guided wave energy at distances larger than 1400 km. We find that the high frequency signals vary gradually with distance, so the effects of this are subdued, and the number of data is still too limited to further restrict the distance range.

For each phase, we consider measurements in four frequency bands: 2 to 4 Hz, 4 to 6 Hz, 6 to 8 Hz, and 8 to 10 Hz. The instrument response was corrected at the center frequency of each passband for all of the phase amplitude measurements. Previous studies have established that rms measures of regional phases like Lg have remarkable stability due to the averaging of multiple arrivals (Gupta *et al.*, 1992; Rodgers *et al.*, 1997a), so we use the pIDC rms amplitude measurements. Noise levels are computed at the pIDC using predicted time and/or group velocity windows around pre-phase noise. In this study only pre-Pn noise is considered as a criterion for selecting the data; events with Pn signal-to-noise ratios greater than two for the frequency bands of interest are retained. This is fairly conservative, given that Pn is usually the weakest regional phase in the data, except when strong Lg blockage occurs (which we do not want to exclude). The number of the selected observations varies with the type of regional phase amplitude measurement observed at each station, ranging between 97 to 109 for NIL, and 66 to 69 for ZAL. The database is growing steadily, and we view our results here as preliminary testing of possible operational implementations with larger data sets.

The paths traversed by our data sample a large area of the Asian continent. Figure 1 shows epicentral locations for the events, station locations, and surface topography in the region. The topographic relief data are from a global digital elevation model developed at the U.S. Geological Survey's EROS Data Center. This database provides a spatial resolution of 30 arc-second (one-km) and an overall vertical accuracy of 70 m (Gesch *et al.*, 1999). Many of the paths traverse mountain ranges such as the Tien Shan, Pamirs and Hindu Kush, high plateaus such as the Iranian and Tibetan Plateaus, or sedimentary basins such as the Tarim Basin. Areas of Lg blockage, inefficient Sn propagation, and low Pn velocities have been reported within our region (e.g., Ni and Barazangi, 1984; Rapine *et al.*, 1997; Rodgers *et al.*, 1997b). Despite the likelihood that internal crustal structure plays an important role in shaping regional seismic phases (Fan and Lay, 1998a,b,c), the available crustal thickness and sediment thickness models for this region were not utilized because they are very low resolution and involve gross extrapolations. We rely on the high resolution topography data to characterize individual path properties. Although variable isostatic compensation and smoothing effects of sedimentation prevent topography from reflecting details of internal crustal structure, to first order topography does indicate gross tectonic features of the crust, with high topography in areas of tectonically thickened crust, and laterally variable topography in areas of rapidly changing crust and mantle structure.

The strategy of empirical correction for parametric path effects is very straightforward. Observed frequency-dependent amplitude ratio measurements for each event recorded by a single station are correlated with various path measurements. High correlations with individual parameters suggest causal influences, but strong covariance amongst parameters mandates a multivariate regression approach to developing a final corrective model. Linear regressions, indicate individual path parameter correlations for Pn/Lg and Pn/Sn ratios measured in different frequency bands at NIL and ZAL. Both amplitude ratios show significant distance dependence, with correlation coefficients ranging between 0.1 and 0.8 at frequencies below 8 Hz. The correlation coefficients and slopes of the linear regressions decrease as frequency increases. The average path parameters considered here are mean elevation (Mean H), topographic variance (Roughness), mean topographic slope (Slope), and the second moment of topography (Skewness) (Zhang *et al.*, 1994). NIL exhibits correlations with these path parameters that can be as strong or stronger than correlations with distance. Mean elevation, average roughness, and, for the higher frequencies, mean slope have linear correlation coefficients of 0.3 to 0.6. ZAL has lower correlations in corresponding cases. NIL has strong negative correlations with skewness of topography, similar to observations at WMQ (Fan and Lay, 1998a,b), while weak positive correlations are found at station ZAL. These correlations in motivate a multivariate regression analysis to account for any collinearity of the path properties.

Assuming an empirical model that minimizes the variance in the data, a best set of predictor variables can be determined from a set of parametric path properties. In practice, the initial list of variables includes the path length and the four path-averaged parameters of topography considered above. Elimination of variables is based on two common criteria: (1) the mean square error (MSE) criterion and (2) the C_p -statistic criterion (Fan and Lay, 1998a). In addition, statistical F-tests help to ensure that the final models have satisfactory estimates of all model coefficients at a high confidence level. Details of this multivariate regression analysis can be found in Fan and Lay (1998a, b, c).

The regression analysis yields models that involve from one to four path parameters. Path length and mean path elevation appear in most of the models, as was found for observations at WMQ (Fan and Lay, 1998 a,b), with surface roughness and rms slope giving some contribution to variance reduction. Figure 2 shows variance

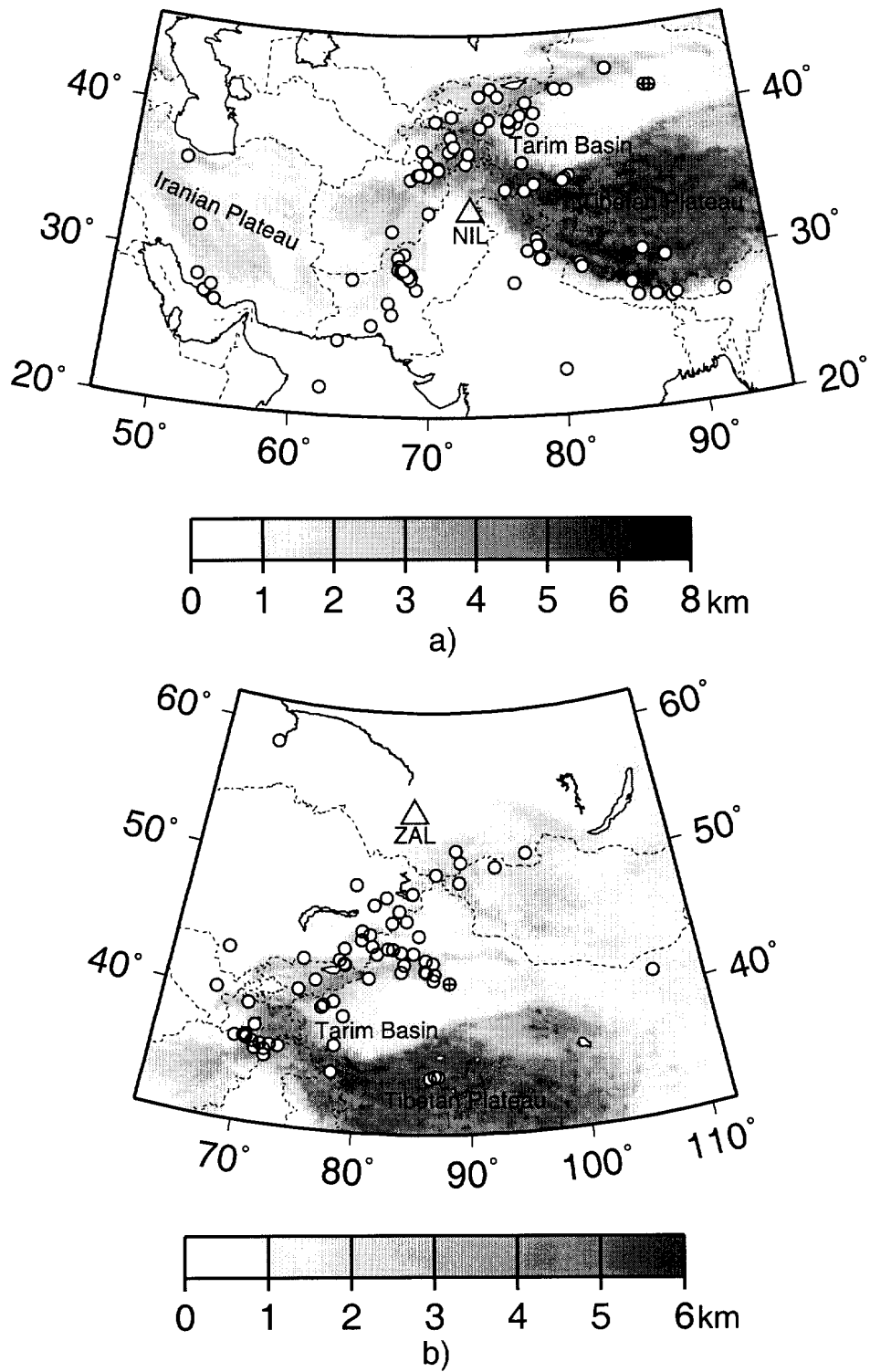


Figure 1. Surface topography in the vicinity of ISMS seismic stations (a) NIL and (b) ZAL. Open circles represents of earthquakes used in this study; circles with a cross are sites of explosions.

reductions achieved by path corrections relative to the raw measurements for NIL and ZAL for four regional discriminant ratios. Known nuclear test signals were omitted. The data for NIL were considered as an entire set (Figure 2a), and in an azimuthal sector spanning azimuths of 0° to 140° (not shown), which straddles the azimuth to the Lop Nor test site. Variance reduction for models involving just distance correction are compared to models with the optimal set of path parameters amongst those considered. It is possible to reduce scatter beyond what is achieved by just distance corrections. For the NIL data, increases in variance reduction by 10-20% beyond distance correction alone are achieved for $\text{Log}(\text{Pn/Lg})$, $\text{Log}(\text{Pn/Sn})$, and $\text{Log}(\text{Pg/Lg})$ amplitude ratios, and there is a few percent improvement for the $\text{Log}(\text{Pg/Sn})$ ratios. The azimuthal subset for NIL shows somewhat stronger distance correction effects than for the whole data set, but there are still significant improvements with the multivariate model. ZAL data experience less variance reduction relative to distance correction alone, involving an extra few percent to 15% (see Figure 2b). The higher frequency windows generally exhibit less dependence on path properties, but path corrections may prove useful across the passband. The low signal-to-noise ratio 8-10 Hz band was found to have very little correlation with topographic parameters, and results for that frequency band are not shown.

Kriging involves spatial multiple regression using a covariance function model Isaaks and Srivastava (1989), and this approach can characterize propagation effects without the need for any information about the waveguide. A spatially damped Bayesian kriging (Schultz *et al.*, 1998) has been used successfully as a predictor of arrival time corrections, with the advantage that it controls estimates in extrapolation zones and allows great flexibility in damping. Rodgers *et al.* (1999) have applied this algorithm to regional phase amplitudes, finding that it outperforms parametric regression approaches. A widely available ordinary kriging algorithm is applied to our data, with the constant mean value being replaced by the location-dependent estimate. An advantage of ordinary kriging is that the sum of the weights is constrained to equal to 1 so ordinary kriging does not require a priori knowledge of the stationary mean for building an estimator, yet it remains unbiased for unsampled values. When applied within a moving data neighborhood, ordinary kriging is a nonstationary algorithm, and it corresponds to a nonstationary random function model with varying mean but stationary covariance. The ability to locally rescale the random function to a different mean value makes ordinary kriging robust. However, extrapolation to poorly sampled areas produces plateaus of varying levels determined by proximate data. Since extrapolation is problematic for all kriging algorithms, this is not seen as a major problem.

We applied ordinary kriging using the $\text{Log}[\text{Pn/Lg}]$ amplitude ratios in the 2-4 Hz frequency band observed at NIL and ZAL. Equal-weighted histograms and cumulative probability plots were created for the Pn/Lg amplitude ratios at each station. Asymmetry of the data histograms suggests that an assumption of normality would be rejected, while the cumulative probability plots indicate that the amplitude ratios are lognormally distributed because the cumulative frequencies plot as a straight line. Kinks in the cumulative probability plots represent changes in the characteristics of the data over different intervals and may be caused by path effects, as suggested by previous studies in which regional discriminants show better normality in distribution after making multivariate path corrections (Fan and Lay, 1998a, b; Rodgers *et al.*, 1999).

The key to successful kriging estimation is choosing a variogram or a covariance that captures the structural pattern of spatial continuity in the data. We first constructed three types of variograms: semivariogram, covariance and correlogram. These variograms typically have been used to describe how spatial variability changes as a function of distance and direction. Variograms were calculated for three experimental directions at angles of 30° , 60° and 90° clockwise from north. The covariance and correlogram display spatial continuity in the data and have few fluctuations because they are resistant to data sparsity, clustering and outlier values. Based on the behavior of these variograms near the origin we select a variogram model for the omnidirectional experimental variogram. The spherical and exponential correlation models are commonly used. We adopt a spherical model to match the experimental variogram for its linear behavior at small separation distances near the origin and its flattening out at larger distances. Isotropic models with a range between 800 and 1200 km resemble the observed semivariograms. Because the range has a relatively minor effect on ordinary kriging weights (Isaaks and Srivastava, 1989), a range of 1000 km is a good choice for our variogram model. The covariance and correlogram also reach a plateau at this distance, confirming that it is appropriate for our data set.

Based on the selected isotropic model, ordinary kriging was performed by searching a regional grid net. To compare estimated values with observed values, we used the cross-validation procedure. As a result of the smoothing effect of kriging, significant variance reduction is achieved. The variance was reduced by 47.1% for the NIL data, and 51.4% for the ZAL data, representing an improvement of 2% (for NIL) and 10% (for ZAL) in comparison to the parametric multiple regression. In addition, the kriging residuals of $\text{Log}[\text{Pn/Lg}]$ for each data set are close to normally distributed populations.

The $\text{Log}[\text{Pn/Lg}]$ ratios clearly display regional coherence, as expected for regionally varying path effects. For NIL low Pn/Lg amplitude ratios are found in Kashmir, close to the seismic station, while high Pn/Lg amplitude ratios are located in the eastern part of the Tibetan Plateau, where strong Lg attenuation or blockage is

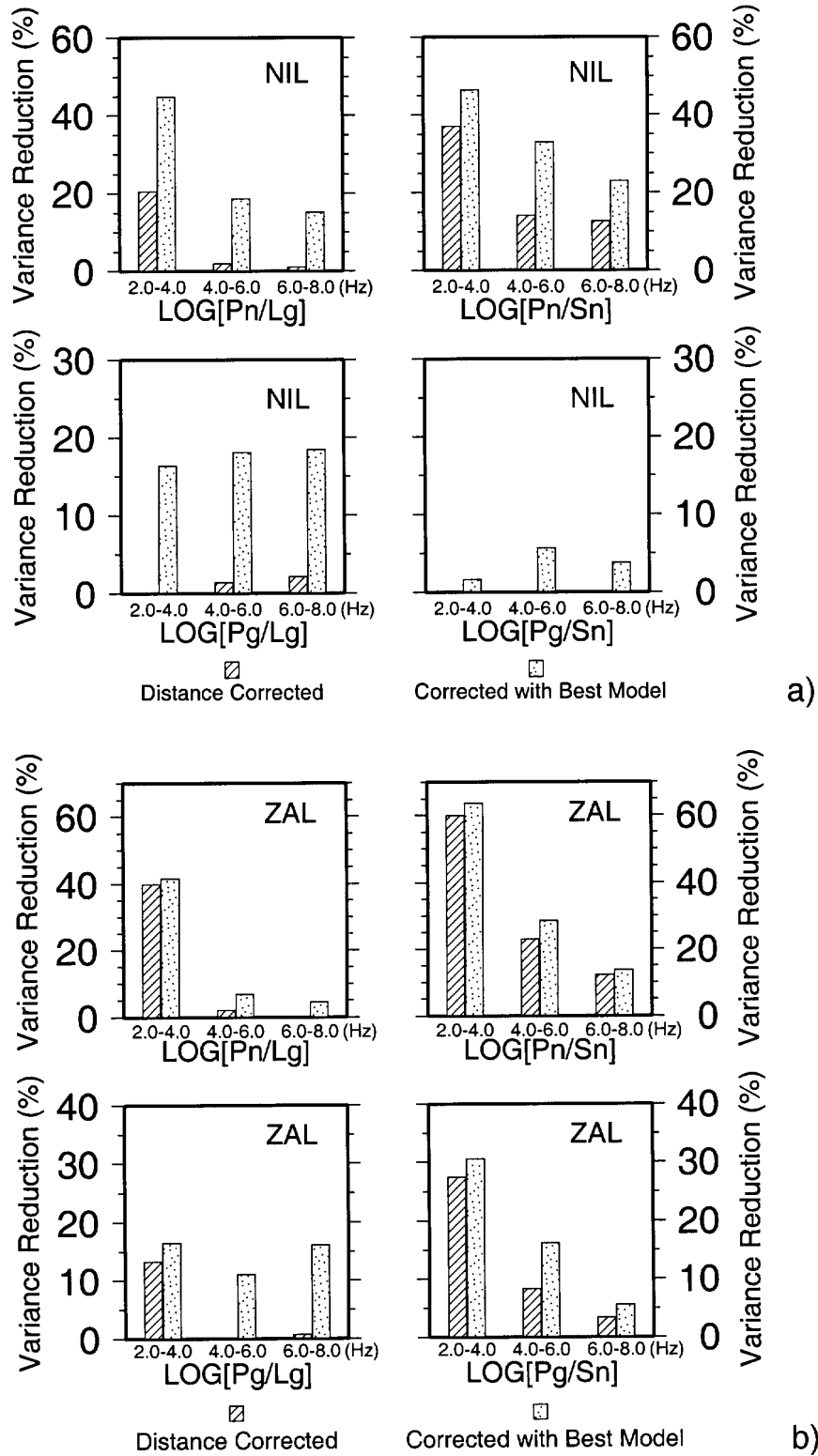


Figure 2. Variance reduction for the Pn/Lg, Pg/Lg, Pn/Sn, and Pg/Sn amplitude ratios achieved at (a) NIL; (b) ZAL. Variance reductions are calculated using corrections for path length only or for the optimal set of parameters in three frequency passbands.

observed (Rapine *et al.*, 1997). A small area between Pakistan and Iran also shows higher $\text{Log}[\text{Pn}/\text{Lg}]$ amplitude ratios. In contrast, at ZAL high Pn/Lg amplitude ratios are found for events in Kashmir, the Pamirs, Hindu Kush, and western Tibet. Low ratios are especially evident for observations from Mongolia and the Baikal rift; these are also regions with low Pg/Lg ratios at LZH (Phillips, 1999). The contrast between regions indicates that the amplitude ratios are controlled by path effects rather than by localized source region effects. This emphasizes the difference in emphasis on path properties between kriging approaches and parametric regressions. Kriging interpolation can predict the value at any point within the grid net based on knowledge of the covariance and values at neighboring points. We expect this to work better for cases where there are many earthquake data near a suspect event, as would be the case here for ZAL, but not NIL. Caution is needed because kriging variance is independent of the data values and usually is not a measure of local estimation accuracy (Journel, 1986).

We now explore whether the separation between earthquake and explosion populations changes after correction for path length and/or other waveguide parameters, i.e., whether the performance of the regional discriminants improves. For our data sets the most effective source discrimination was found for Pn/Lg ratios at NIL. Figure 3 shows $\text{Log}(\text{Pn}/\text{Lg})$ values as a function of event magnitude for three frequency passbands. Two explosion events at the Lop Nor test site in China are well isolated in the 2-4 Hz and 6-8 Hz frequency bands. In the 4-6 Hz band an earthquake overlaps the explosion group. This event is an outlier of the earthquake population, and is located south of the Tibetan Plateau with a path traveling along the Plateau margin. Distance corrections result in reduced variance as shown in the middle row of Figure 3, but there is little influence on the separation between the earthquake and explosions populations (given the small number of explosion observations, we do not attempt to apply statistical tests, but simply rely on visual separation). Path correction using the best models from multivariate regression analysis (lower row of Figure 3) provides further improvement in variance reduction and better source discrimination in all three passbands in this case. This is the ideal goal for path corrections, to tighten up the scatter in the reference earthquake population while enhancing the separation of the explosion population.

Similar behavior is observed for the $\text{Log}(\text{Pg}/\text{Lg})$ measurements at NIL. Complete sample separation between earthquake and explosion populations is only found for the frequency band of 2-4 Hz, but the path corrections do give significant improvement in population separation in the two higher bands. The regional discriminants that involve Lg at NIL are more effective for source discrimination at lower frequency. Path corrections for the $\text{Log}(\text{Pn}/\text{Sn})$ ratios also provide significant variance reduction, however, better separation of earthquake and explosion populations is found at higher frequencies.

While not shown here, the discrimination performance for NIL is enhanced by considering the azimuthally restricted subset. Despite the fact that the overall variance reduction of path corrections is no stronger, there is clearer separation of earthquake and explosion populations than for the complete data set. We believe that there are two factors responsible for this. One is that several earthquakes with particularly strong path effects involving Lg blockage were excluded in the azimuthally limited data. Another factor is that by restricting the azimuthal coverage the data experience more similar travel paths, resulting in more effective path corrections.

Discriminant measurements at ZAL do not perform as well as those at NIL, even though the available explosion sources are located in the same source region. Figure 4 shows the observations for $\text{Log}(\text{Pn}/\text{Lg})$. The substantial overlap between earthquake and explosion populations is presumably a result of strong path effects. Correction for path length reduces the overlap, but does not achieve separation between earthquake and explosion populations. Using the best parametric regression provides slight further improvement in source discrimination for $\text{Log}(\text{Pn}/\text{Sn})$, but has little effect on $\text{Log}(\text{Pn}/\text{Lg})$. Other stations, such as AAK also do not provide clean discrimination (Hartse *et al.*, 1998). In some instances kriging may do better than the parametric regressions, but this involves a large extrapolation for station NIL, and the coverage is very one-sided for ZAL.

CONCLUSIONS AND RECOMMENDATIONS

In this study we made path corrections for regional seismic discriminants observed at two CTBT monitoring stations in Asia. Correction of the path effects is based on empirical models derived from multivariate regression analysis and ordinary kriging. The parametric multiple regression uses a high-resolution topographic database to develop corrections involving path length and/or other topographic parameters. The corrections reduce the variance in the regional discriminants, particularly at lower frequencies. Kriging outperforms the multivariate regression approach in terms of reducing the earthquake population variance. For station NIL, the path corrections enhance discrimination effectiveness for a small set of explosions, while for station ZAL there is improvement, but still substantial overlap of the populations. This variation in discriminant performance presumably reflects acute waveguide heterogeneity that is not captured in the parametric regression analysis. Accumulating larger data sets, with improved sampling of the paths traversed

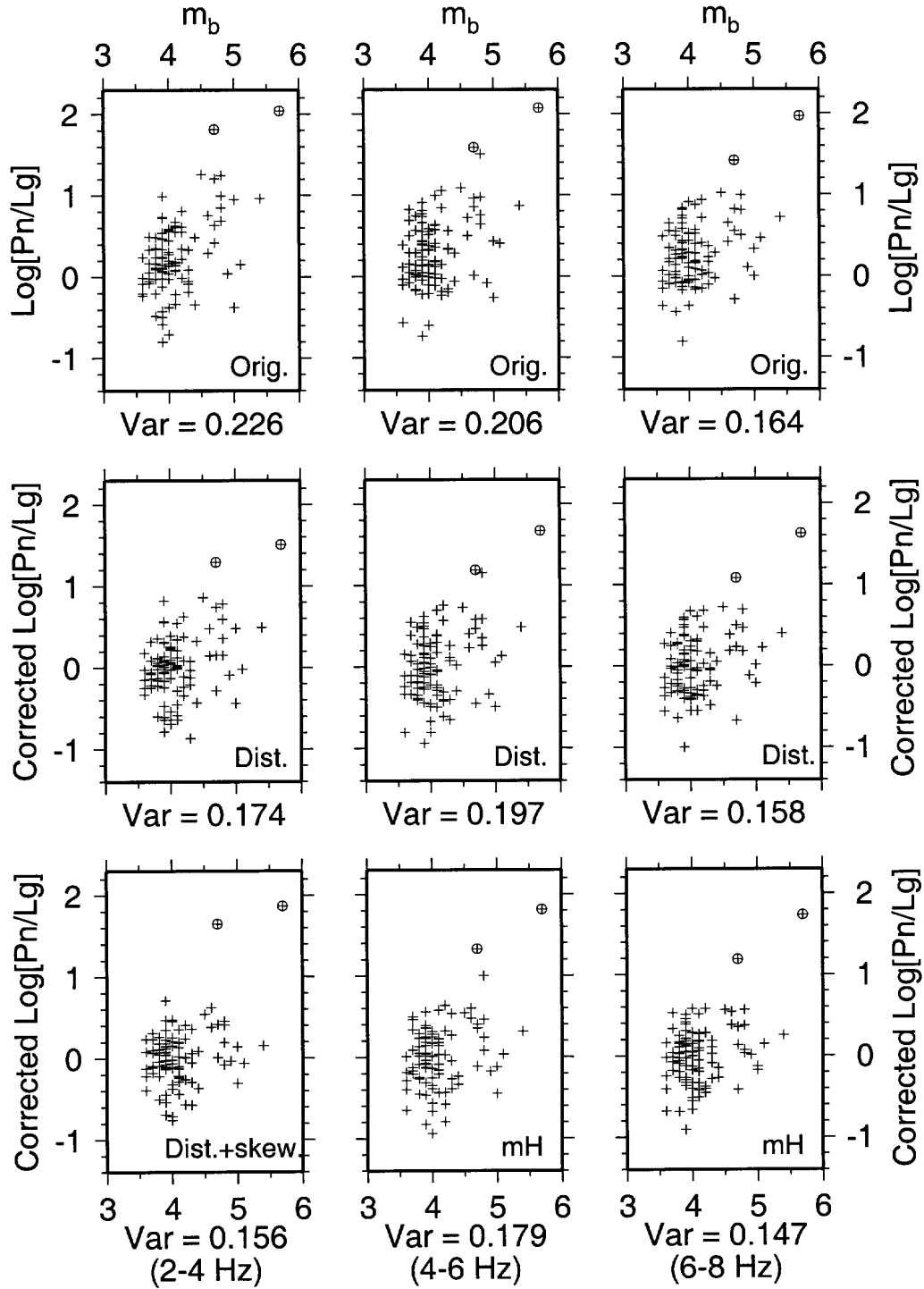


Figure 3. $\text{Log}[Pn/Lg]$ measurements observed at NIL as a function of event magnitude in uncorrected form (top row) compared with those measurements corrected for path length (middle row) or for the optimal set of topographic parameters (bottom row) in three frequency passbands. Orig., observed data; Dist., corrected for path length; mH, corrected for mean altitude; Dist.+skew., corrected for a two-parameter model involving distance and skewness of topography.

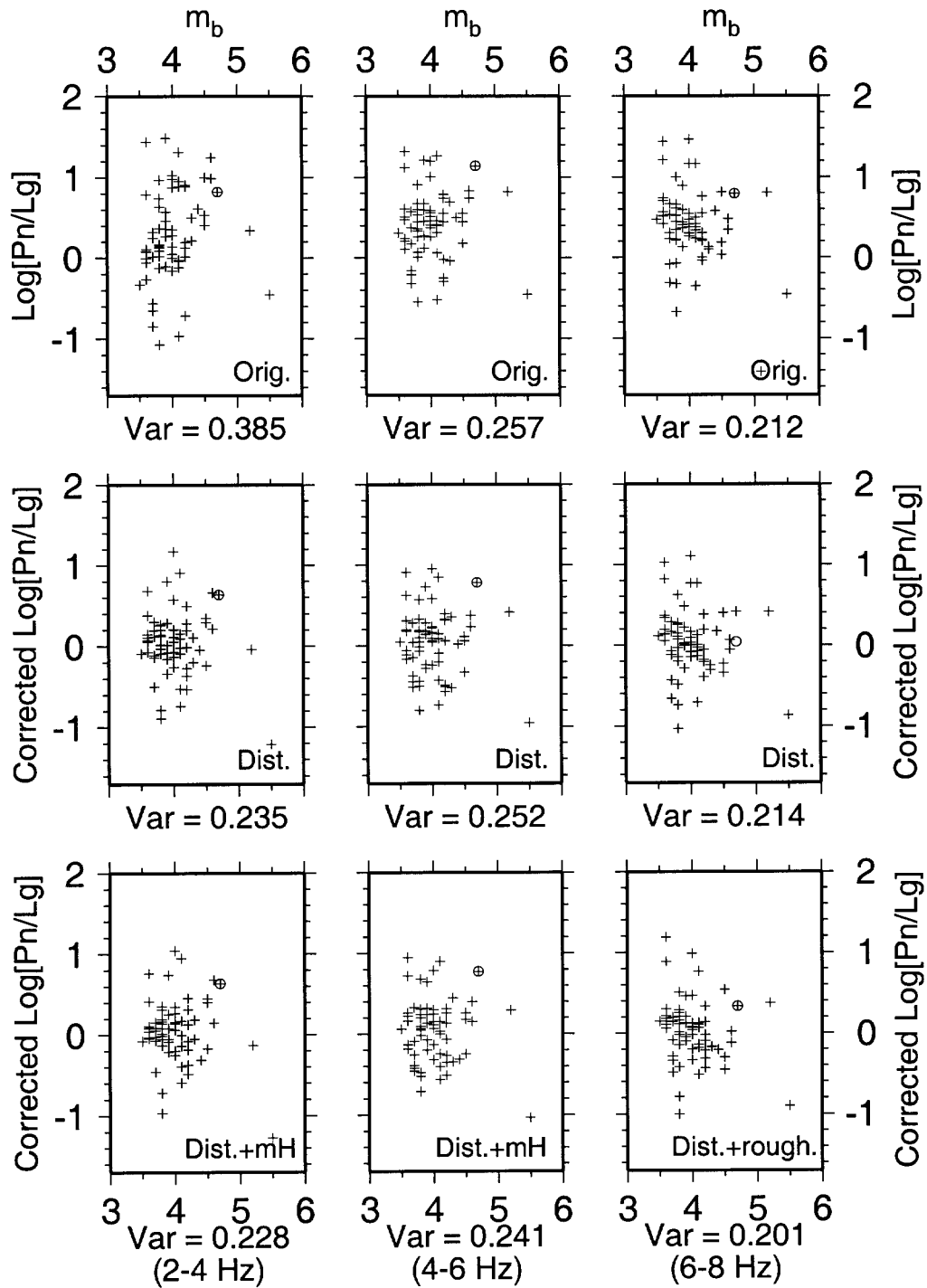


Figure 4. $\text{Log}[Pn/Lg]$ measurements observed at station ZAL, plotted as a function of event magnitude, for uncorrected form (top row), distance corrected data (middle row) and multivariate regression corrected data (bottom row). Dist.+mH, corrected for a two-parameter model involving distance and mean path elevation along the path; Dist.+rough., corrected for a two-parameter model involving distance and average topography roughness.

by explosion signals, would likely lead to superior performance for both stations. Improved coverage would also reduce the degree of extrapolation currently required for the kriging analysis to be applied to the specific explosion source region in western China. Overall, there is a promising indication that application of propagation corrections is beneficial for these regional discriminants, but further work is needed to establish a preferred operational approach.

REFERENCES

- Fan, G.-W., and Lay, T., (1998a), Statistical analysis of irregular waveguide influences on regional seismic discriminants in China, *Bull. Seism. Soc. Am.*, 88, 74-88.
- Fan, G.-W., and Lay, T., (1998b), Regionalized versus single-station wave-guide effects on seismic discriminants in western China, *Bull. Seism. Soc. Am.*, 88, 1260-1274.
- Fan, G.-W., and Lay, T., (1998c), Statistical analysis of irregular waveguide influences on regional seismic discriminants in China: additional results for Pn/Sn, Pn/Lg and Pg/Sn, *Bull. Seism. Soc. Am.*, 88, 1504-1510.
- Gesch, D.B., Verdin, K.L., and Greenlee, S.K., (1999), New land surface digital elevation model covers the Earth, *EOS Trans., AGU*, 80, 69-70.
- Gupta, I.N., Chan, W.W., and Wagner, R.A., (1992), A comparison of regional phase from underground nuclear explosions at East Kazakh and Nevada test sites, *Bull. Seism. Soc. Am.*, 82, 352-382.
- Hartse, H.E., Flores, R.A., and Johnson, P.A., (1998), Correcting regional seismic discriminants for path effects in western China, *Bull. Seism. Soc. Am.*, 88, 596-608.
- Isaaks, E.H., and Srivastava, R.M. (1989), *An Introduction to Applied Geostatistics*, Oxford University Press, New York.
- Journel, A.G. (1986), Geostatistics: Models and tools for the Earth sciences, *Math. Geol.*, 18, 119-140.
- Ni, J., and Barazangi, M., (1983), High-frequency seismic wave propagation beneath the Indian Shield, Himalayan Arc, Tibetan Plateau and surrounding regions: high uppermost mantle velocities and efficient S_H propagation beneath Tibet, *Geophys. J. R. astr. Soc.*, 72, 665-689.
- Phillips, W.S., (1999), Empirical path corrections for regional phase amplitudes, *Bull. Seism. Soc. Am.*, 89, 384-393.
- Rapine, R.R., Ni, J. F., and Hearn, T.M., (1997), Regional wave propagation in China and its surrounding regions, *Bull. Seism. Soc. Am.*, 87, 1622-1636.
- Rodgers, A.J., Lay, T., Walter, W.R., and Mayeda, K.M., (1997a), A comparison of regional phase amplitude ratio measurement techniques, *Bull. Seism. Soc. Am.*, 87, 1613-1621.
- Rodgers, A.J., Ni, J.F., and Hearn, T.M., (1997b), Propagation characteristics of short period S_H and L_g in the Middle East, *Bull. Seism. Soc. Am.*, 87, 396-413.
- Rodgers, A.J., Walter, W.R., Schultz, C.A., Myers, S.C., and Lay, T., (1999), A comparison of methodologies for representing path effects on regional P/S discriminants, *Bull. Seism. Soc. Am.*, 89, 394-408.
- Schultz, C.A., Myers, S. C., Hipp, J., and Young, C.J., (1998), Nonstationary Bayesian Kriging: A predictive technique to generate spatial corrections for seismic detection, location and identification, *Bull. Seism. Soc. Am.*, 88, 1275-1288.
- Zhang, T.-R., Schwartz, S., and Lay, T., (1994), Multivariate analysis of waveguide effects on short-period regional wave propagation in Eurasia and its application in seismic discrimination, *J. Geophys. Res.*, 99, 21,075-21,085.